# 150-W Power-Over-Fiber Using Double-Clad Fibers

Motoharu Matsuura, *Senior Member, IEEE*, Nana Tajima, Hayato Nomoto, and Daisuke Kamiyama

*(Top-Scored Paper)*

***Abstract*—This article presents simultaneous data and power transmission systems using a double-clad fiber (DCF). In future radio-over-fiber (RoF) networks, a large number of remote antenna units (RAUs) will be required to provide various kinds of mobile communication services. Power-over-fiber (PWoF), which delivers electrical power to drive the RAUs in optical fibers, is an attractive technique that offers cost-effective installation, operation, and maintenance of RAUs, and achieves the power savings across the entire RoF networks. In particular, the use of double-clad fibers (DCFs), which consist of a single-mode (SM) core and an inner cladding that surrounds the SM core, are useful for much higher power transmission than conventional PWoF techniques. Along the DCF link, optical data signals are transmitted into the SM core, whereas high-power feed light for optical powering is transmitted into the inner cladding, which has a core area that is approximately 240 times larger core area than that of conventional SM cores. In this article, we experimentally demonstrate a PWoF feed with up to 150-W of power using a 1-km DCF. To show the feasibility of the PWoF system, we investigate the bend performance and temperature characteristics of the DCF link. We also evaluate data and power transmission performance under the 150-W PWoF feed in the DCF link.**

***Index Terms*—Double-clad fibers (DCFs), mobile communications, optical power delivery, power-over-fiber (PWoF), radio-over-fiber (RoF), remote antenna units (RAUs).**

## I. Introduction

OPTICAL transmission systems are expected to play an important role in supporting multiple wired and wireless internet services in future communication networks [1], [2]. In particular, radio-over-fiber (RoF) is an essential technology for transmitting radio-frequency (RF) signals into fiber links between a central office (CO) and remote antenna units (RAUs), as well as for providing broadband mobile communications [3]–[5]. A reduction in the cell size of RAUs is required to support higher data rates for RF signals, and a large number of RAUs should be installed, especially in densely populated areas. Therefore, it is important to provide cost-effective installation, operation, and maintenance of RAUs.

Power-over-fiber (PWoF) is a simple way to simultaneously transmitting optical data and power into the same optical fiber. In RoF networks, PWoF is effectively used not only to deliver the power required for driving RAUs from a CO, but also to centralize the power source in the CO. Although it is well known that the power transmission efficiency (PTE) of PWoF is lower than that of conventional electrical power lines, we believe that PWoF is an attractive approach to reducing overall network power consumption. For example, in conventional RAUs, full driving power is supplied on the assumption that each RAU enables us to support not the "actual" traffic load but the "maximum" traffic load. Therefore, the network consumes a large amount of unnecessary driving power. To solve this problem, a few research groups have shown that the introduction of "sleep mode" power control, which is a low power mode for electric devices of the RAUs, offers a power savings of up to 60% in the mobile networks [6]–[8]. On the other hand, as PWoF makes it possible to manage the power supplied to the RAUs by controlling the output power of the feed light source in the CO, it is easy to adjust the power with finer granularity in response to the temporary traffic load of each RAU [9]. "Sleep mode" is generally used as only midnight power supply systems, whereas the dynamic power control by PWoF is useful for temporally optimizing the supplied power in all the day. If power can be precisely modulated over the variations in traffic load, it is expected that the overall network power consumption will be efficiently reduced. In this scheme, the power supply equipment except for photovoltaic power converters (PPCs), which convert optical power into electrical power, can be removed from the RAUs. Therefore, it will be possible to greatly simplify the configuration and power supply equipment of the RAUs.

As optical fibers are nonconductive power lines, unlike electrical cables, PWoF is useful for avoiding lightning damage to the electrical equipment connected to optical fibers, such as the COs. However, the power that is required to drive a conventional small-cell-type RAU spans at least several watt classes. Single-mode fibers (SMFs) are not suitable for high-power feed because the small core area strictly limits the available feed light power [10]. Multimode fibers (MMFs) are pre-existing fibers that do not require a large-scale deployment of new fibers, and have a larger core area than SMFs. However, the

Manuscript received May 31, 2019; revised July 25, 2019, September 6, 2019, and October 12, 2019; accepted October 18, 2019. Date of publication October 21, 2019; date of current version January 23, 2020. This work was supported in part by the Grant-in-Aid Scientific Research from the Ministry of Education, Culture, Sports, Science, and Technology (17H03260) and in part by the Telecommunication Advancement Foundation in Japan. *(Corresponding author: Motoharu Matsuura.)*

M. Matsuura and H. Nomoto are with the Graduate School of Informatics and Engineering, University of Electro-Communications, Tokyo 182-8585, Japan (e-mail: m.matsuura@uec.ac.jp; h.nomoto@uec.ac.jp).

N. Tajima and D. Kamiyama were with the Graduate School of Informatics and Engineering, University of Electro-Communications, Tokyo 182-8585, Japan. They are now with the NTT Docomo, Inc., Tokyo 100-6150, Japan (e-mail: nana-tajima@uec.ac.jp; daisuke.kamiyama@uec.ac.jp).

Color versions of one or more of the figures in this article are available online at http://ieeexplore.ieee.org.

Digital Object Identifier 10.1109/JLT.2019.2948777

transmission speed of MMF links is strictly limited owing to modal dispersion [11], [12]. In addition, there exists crosstalk between the high-power feed light and the data signals, which are significantly weaker and very sensitive to variations in the intensity of the feed light that is in the same core of MMF link transmission [13], [14].

To date, we have reported the PWoF technique using double-clad fibers (DCFs), which consist of a single-mode (SM) core and an inner cladding that surrounds the SM core [9], [15]–[25]. In the DCF links, the optical data signals were propagated in the SM core without modal dispersion, whereas the high-power feed light was delivered through the inner cladding with a core effective area that was greater than that of the SM core. As our representative achievements, we demonstrated PWoF experiments with good transmission performances for bidirectional RoF transmission [9], [15]–[18] and multi-channel transmission at 1.3 $\mu$m [19] and an optically controlled beam steering system over a 300-m DCF link [20]. Also, we have achieved multichannel analog and digital data transmission and delivered up to 7-W electrical power over the DCF link [21], [22]. Moreover, we have observed no significant crosstalk between data signals and feed light for single-channel, bidirectional RoF transmission over 1-km DCF link [23]. However, in these studies, the maximum PWoF feed power is up to 60 W, and it is necessary to evaluate the transmission performance of data signals and the characteristics of the key components of DCF links in higher PWoF feed power transmission.

In this study, we focus on exploring the possibilities of the PWoF technique using DCFs for 150-W power feed, which is much higher than those of the presented PWoF experiments so far. While preliminary results have been presented in Ref. [24], in this work we include the investigation of the characteristics of the key components of the DCF link and discuss the performances in detail. First, to show the practicability of DCFs, we measured the bend performance of the DCF we used in this experiment. Also, to investigate the influence of high-power feeding on DCF links, we measure the temperature characteristics of a 1-km DCF link when the feed light enters the DCF link at power levels up to 150 W. Lastly, we evaluate the bidirectional transmission performance of optical data signals over the DCF link under the 150-W PWoF feed.

This paper is organized as follows. In Section II, we describe the experimental setup for evaluating the power and data transmission performance of a 1-km DCF link. In Section III, we describe the bend performances of the DCF we used in the experiments that follow. In Section IV, we evaluate the optical and electrical power transmission performance of the 1-km DCF link. In Section V, we describe the temperature characteristics over a time interval of 10 min in the 1-km DCF link when the feed light enters it at a power level as high as 150 W. In Section VI, we evaluate the bidirectional transmission performances of the downlink- and uplink-transmitted data signals in terms of error-vector magnitude (EVM) measurements. In Section VII, we discuss the potentials for realizing the improved performance of the presented system and its related applications. Section VIII concludes the paper.

## II. Experimental Setup

Fig. 1 shows the experimental setup for the 150-W PWoF feed experiment using a 1-km DCF link between a CO and an RAU. In this scheme, there are two transmitter-receiver pairs for bidirectional transmission. In the downlink transmitter, an optical analog data signal with a wavelength of 1550 nm was generated by a laser-diode (LD) and a $LiNbO_3$ modulator (LNM) for external modulation. A polarization controller (PC) at the output of the LD was employed to adjust the state of the polarization of the data signal in order to obtain the highest signal quality at the output of the LNM. Electrical data for generating the data signal was based on the IEEE 802.11a wireless local area network (WLAN) standard using 64-quadrature amplitude modulation (64-QAM) and orthogonal frequency-division multiplexing (OFDM) format. The electrical data with a carrier frequency of 5.2 GHz were generated by a signal generator (SG) (MS2830A, Anritsu Corp.). Although this data format is mainly used for conventional WLAN systems rather than latest mobile communications, we believe that the difference is not significant in the crosstalk between optical data signals and feed light under high optical power feed. An isolator (ISO) was used to remove the signal degradation due to reflection noise in the signal. Then, an erbium-doped fiber amplifier (EDFA) was used to adjust the signal power level. A band-pass filter (BPF) with a 3 dB bandwidth of 0.6 nm was used to remove the amplified spontaneous emission noise emitted by the EDFA. In the uplink transmitter, an optical analog data signal that was the same as the downlink signal was generated. These data signals were simultaneously transmitted into the 1-km DCF link, which included the circulators (Circ.), cladding power strippers (CPSes), and tapered fiber bundle combiner (TFBC) and divider (TFBD). At each receiver, the transmitted signals were converted into the electrical signals by using photo-diodes (PDs). After adjusting the signal power injected into the signal analyzers (SAs) by using variable attenuators (ATTs), the qualities of the transmitted signals were measured by the SAs in terms of EVM and spectrum emission mask (SEM) measurements. In the uplink receiver, an EDFA and the following BPF were intentionally located in front of the PD in order to reduce the power consumption of the RAU as much as possible. For the feed light sources employed to optically power the RAU, we used four commercially available 808 nm high-power LDs (HPLDs) (LIMO35-F100-DL808-LM, LIMO Ltd., and K808DA5RN-35.00W-SMA905, BTW Ltd.), which had a maximum output power of 35 and 40 W, respectively. The output fibers of the HPLDs were step-index multimode fibers (MMFs) with a core diameter of 105 $\mu$m. The data signals and the four feed lights were combined using the $(4 \times 1) + 1$ TFBC and transmitted into the 1-km DCF. The CPS was used to eliminate the reflected feed lights in the inner cladding of the DCF link. The DCF consisted of an SM core with a core diameter of 8 $\mu$m and an inner cladding with a core diameter of 125 $\mu$m. Although the outer cladding diameter was 180 $\mu$m, the actual DCF was a bare fiber with an outer fiber diameter of 250 $\mu$m, including the polymer coating. By employing the TFBC, the data signal was injected into the SM core, whereas the four feed

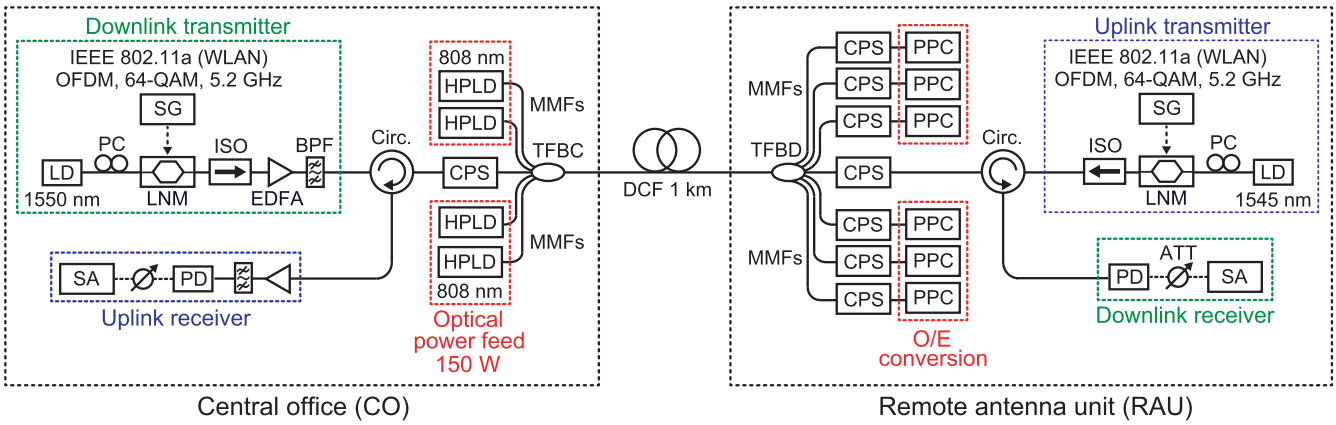


Fig. 1. Experimental setup for 150-W PWoF feed experiment using a 1-km DCF. LD: laser-diode, PC: polarization controller, LNM: $LiNbO_3$ modulator, SG: signal generator, ISO: isolator, EDFA: erbium-doped fiber amplifier, BPF: bandpass filter, Circ.: Circulator, CPS: cladding power stripper, HPLD: high-power laser-diode, MMF: multimode fiber, TFBC: tapered fiber bundle combiner, TFBD: tapered fiber bundle divider, PPC: photovoltaic power converter, PD: photo-diode, ATT: electrical attenuator, SA: signal analyzer.

lights were injected into the inner cladding of the DCF through the four tapered MMFs. After transmission, the $1 \times (6 + 1)$ TFBD was used to divide the data signal and feed lights. The TFBD had one DCF input and one DCF and six MMF outputs with a core diameter of 105 $\mu$m. The feed light was extracted from the inner cladding of the DCF through the six tapered MMFs. The feed light power transmitted into each MMF output was injected into each photovoltaic power converters (PPCs) to convert the optical power into electrical power. The PPCs were commercially available devices (YCH-H003-15-FC, MH GoPower, Ltd.) [26], [27]. The maximum input power and the optical-to-electrical (O/E) conversion efficiency were 10 W and approximately 24% at a wavelength of 808 nm, respectively. In the RAU, the CPS, which consisted of the DCF input and the SMF output, was used to eliminate the transmitted feed lights in the inner cladding of the DCF in order to prevent damage due to high-power feed light injection into the downlink receiver.

## III. Bend Performance of Double-Clad Fibers

The bend loss of optical fibers is an important issue, especially in high-power fiber transmissions such as PWoF, because the power loss degrades the power transmission performance and may cause thermal damage to the fiber [28]. In particular, the inner claddings of DCFs have a thinner outer cladding than those of any other fiber, as mentioned in the previous Section. To confirm the influence of the bend loss on the power transmission performance of the DCFs, we measured the bend performance of the inner cladding of the DCF we used.

Fig. 2(a) shows the experimental setup for the bend performance measurement. As a test light source, we used one of the HPLDs used in the 150-W PWoF experiment, as shown in Fig. 1. The wavelength and output power of the HPLD were 808 nm and 1 W, respectively. Although the test fiber was the same DCF as in the 150-W PWoF experiment, the total length was 100 m. The DCF had a polymer coating of curable resin that formed a diameter of 250 $\mu$m as well as conventional SMFs and MMFs. In

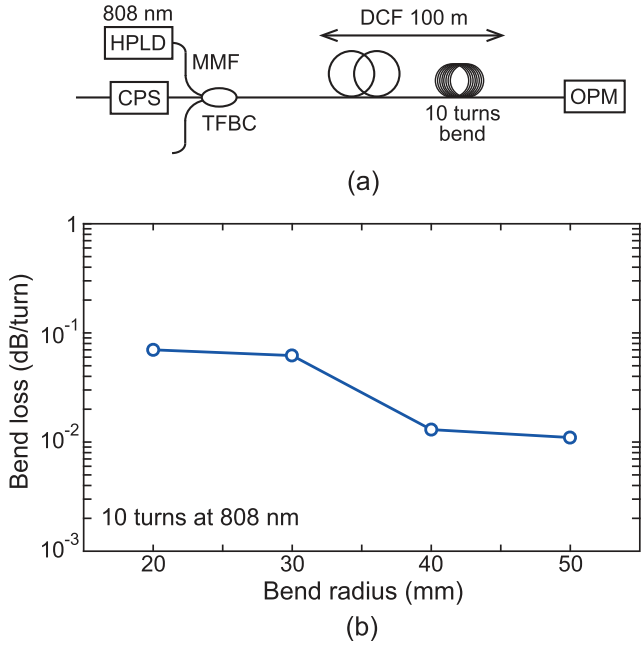


Fig. 2. (a) Experimental setup for bend performance measurement. (b) Bend loss of inner cladding of DCF while changing bend radius.

this measurement, one part of the 100-m DCF was bent around mandrels with various bend radii from 20 mm to 50 mm, and the bend was based on 10 iterations of full 360° turns and kept under slight tension to remove any slack.

The test light was injected into the inner cladding of the DCF through the TFBC. After transmission with and without fiber bending, the output power of the test light was measured and compared using an optical power meter (OPM).

The measured bend loss of the inner cladding of the DCF is shown in Fig. 2(b). Here, the bend loss is defined as the additional loss when the fiber is bent. As the bend radius became smaller, the bend loss was increased. However, the bend losses were less than 0.07 dB/turn, even when the bend radius was reduced

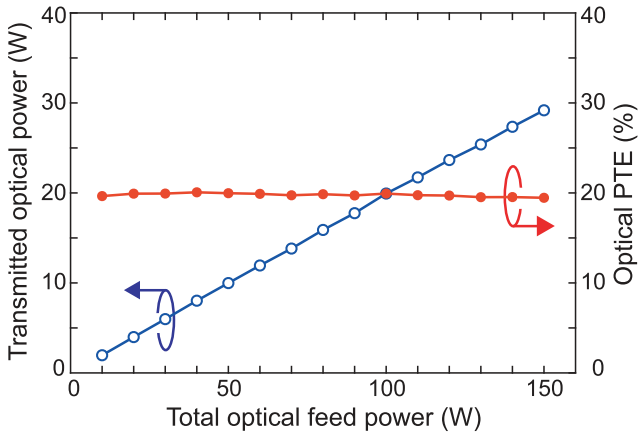


Fig. 3. Transmitted optical power and PTE as a function of total optical feed power.

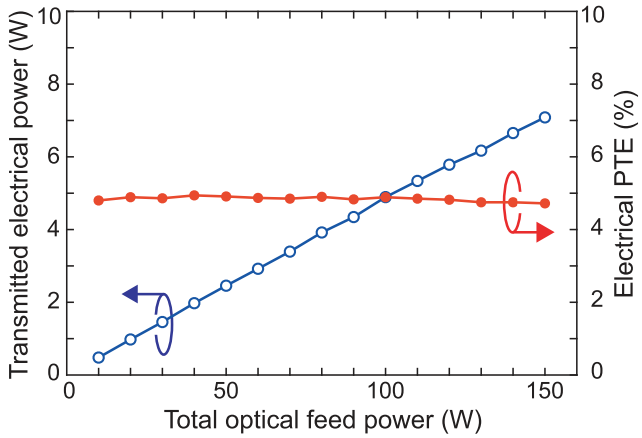


Fig. 4. Transmitted electrical power and PTE as a function of total optical feed power.

to 20 mm. This result shows that the DCF has high tolerance for tight bends and would be feasible for practical use in real deployment.

## IV. Optical and Electrical Power Transmission Efficiencies

To evaluate the power transmission performance (PTE) of the DCF link, we measured the transmitted optical power to the PPC inputs and the PTE, which is defined as the power ratio between the two HPLD outputs and the six PPC inputs. The result is shown in Fig. 3. As the total optical feed power increased, the transmitted optical power linearly increased, and the PTE was almost constant. This means that there was no critical power loss (absorption) dependence on the feed power injected into the DCF link. The calculated average PTE was approximately 19.70%. For example, in the 150-W optical feeding, the transmitted optical power and the PTE were 29.1 W and 19.46%, respectively. In this scheme, the estimated losses of the TFBC, TFBD, CPS at the input of the PPCs were 1.0 dB, 1.5 dB, and 1.25 dB, respectively. The transmission loss of the inner cladding of the DCF at the wavelength of 808 nm was approximately 3.3 dB/km.

Next, to evaluate the electrical power supply capability of the PWoF system, we measured the electrical PTE, which is defined as the power ratio between the two HPLD outputs and the total electrical power converted by the six PPCs. The result is shown in Fig. 4. As the total optical feed power increased, the converted electrical power increased linearly, whereas the PTE was almost constant regardless of the total optical feed power. Power linearity and the constant PTE are quite useful in the control of supplied power according to the temporary traffic load of each RAU, as mentioned in Section I. In the 150-W optical feed, the total transmitted electrical power was 7.08 W. The calculated average PTE was approximately 4.84%. The low PTE resulted mainly from the 808-nm feed light wavelength, which was outside the suitable wavelength band (900 nm to 970 nm) that is required to obtain the highest O/E conversion efficiency for the PPCs [26]. If we were to use PPCs with a higher O/E conversion efficiency, the PTE would be further improved.

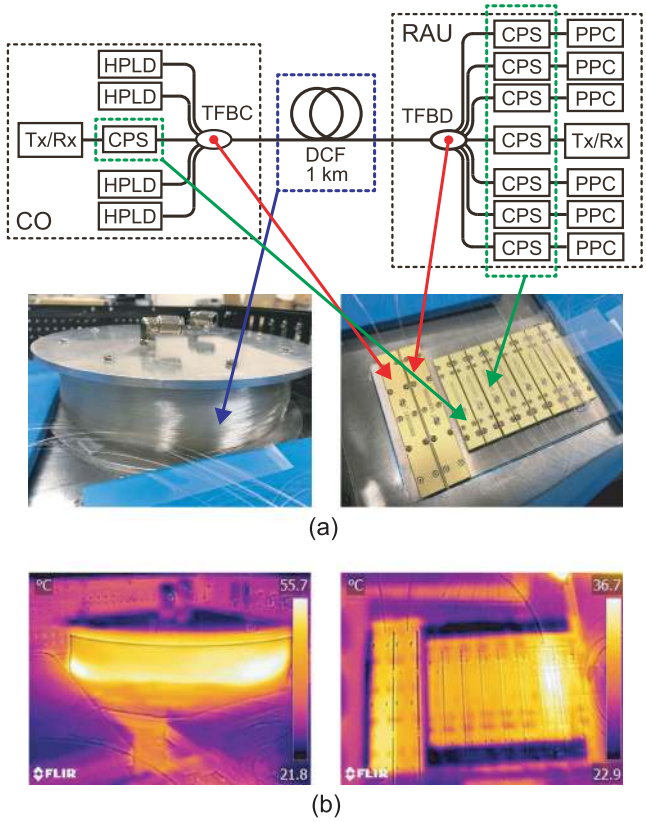


Fig. 5. (a) Experimental setup and photos of main components of PWoF system. (b) Examples of thermographic photo images.

## V. Temperature Characteristics

In PWoF systems with a high-power optical feed, the heat induced by the transmission loss into the PWoF link, including optical components such as TFBC, CPS, and TFBD, may have some effect on the reliability and long-term signal and power transmission performance for the PWoF systems. Therefore, we measured the temperature change in the PWoF system. Fig. 5(a) shows a simplified experimental setup and photos of the main

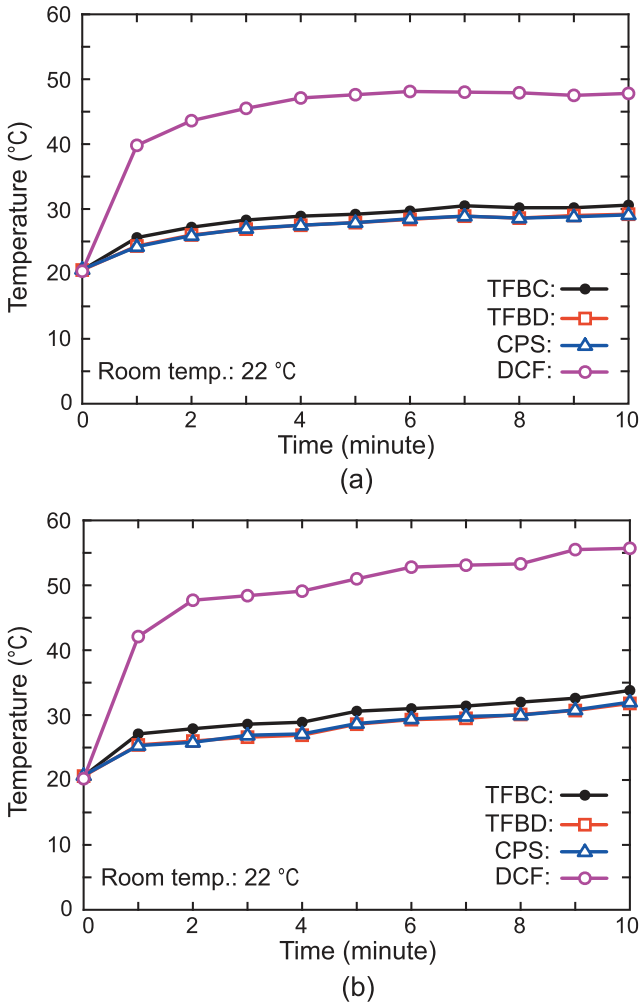


Fig. 6. Temperature changes in main components in 10 minutes in (a) 120-W and (b) 150-W PWoF feed in 1-km DCF link.

components of the PWoF system. The experimental setup used the same configuration as the 150-W PWoF experiment, as shown in Fig. 1. For this measurement, we did not use any active cooling systems for the PWoF scheme, such as fan cooler and water cooler. Examples of the thermographic photo images of the components are shown in Fig. 5(b). The temperatures were measured using a commercially available thermal camera (FLIR C2, FLIR Systems, Inc.). The photos show that the difference in temperature is indicated by the difference in color.

Fig. 6 shows the temperature changes in the main components of the 1-km DCF PWoF system over a 10 minutes period. In this experiment, the room temperature was 22 °C. The temperatures were measured at the highest temperature part of each component. In the 120-W PWoF feed, as shown in Fig. 6(a), the temperatures of the TFBC, TFBD, and CPSs rose slightly over the time. On the other hand, the DCF reached a much higher temperature than the other components, because the DCF was bent around a drum, as shown in the left picture of Fig. 5(a). In this case, the heat induced by the transmission loss of the long DCF accumulated in the DCF drum. However, in real deployment, it is easy to diffuse the heat, because DCFs are

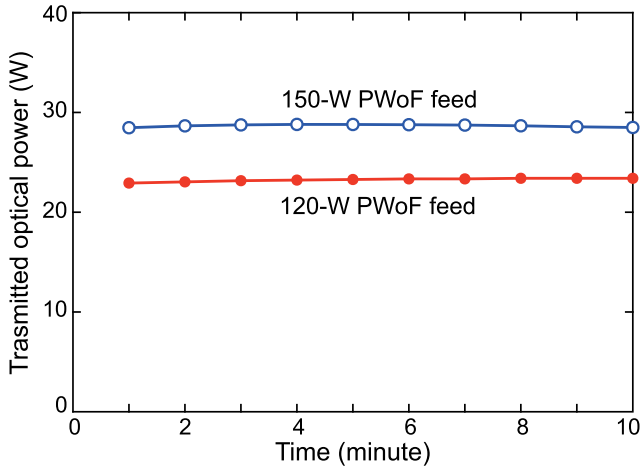


Fig. 7. Transmitted optical power over 10 minutes in 120-W and 150-W PWoF feed.

installed in a straight line without bending around drums. Furthermore, it was observed that the temperatures remained almost constant after 7 minutes in all the cases. Fig. 6(b) shows the temperature changes in the 150-W PWoF feed. The rises in temperature were slightly larger than for 120-W PWoF feed, and the temperatures did not tend toward a constant value after 10 minutes. We think that this is related to the measuring time and the cooling capability of the DCF link. In this scheme, we did not use any active cooling systems for the DCF link. In addition, there were maximum input powers of the TFBC, TFBD, and CPSs although the upper limits were not exceeded in this experiment. For these reasons, it was difficult to completely suppress the temperature rise in the 150-W PWoF feed within 10 minutes. Since the temperature rise in the 150-W PWoF feed was not so large, it is expected that the temperature will tend toward a constant value if the temperature is measured for a longer time or we use TFBC, TFBD, and CPSs with higher power handlings.

To investigate the stability of the power transmission performance of the PWoF system under a high-power feed, we measured the transmitted optical power over 10 minutes in the 120-W and 150-W PWoF feeds. The result is shown in Fig. 7. Although the temperatures of all the components of the PWoF system slightly rose over time, as shown in Fig. 6, there were almost no change in the transmitted optical power. The variations were less than 1.5%. It was thus found that the high-power feed had no influence on the power transmission performance within the temperature change shown.

## VI. Bidirectional Transmission Performance

To evaluate the bidirectional data transmission performance of the entire system under a high-power feed, we measured the EVM characteristics of the downlink- and uplink-transmitted signals and compared the performance of the back-to-back signal. Fig. 8 shows the EVM curves of the back-to-back and transmitted signals, with and without the 150-W PWoF feed, as a function of the received electrical signal power. As the received power was increased, the EVM values decreased. When

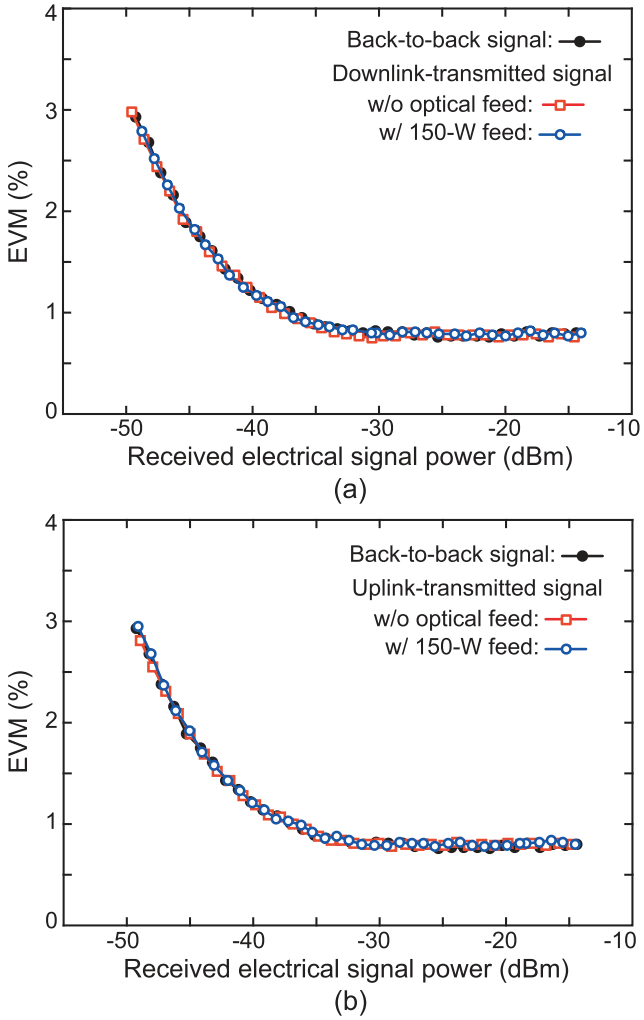


Fig. 8. EVM curves of (a) back-to-back and downlink-transmitted and (b) back-to-back and uplink-transmitted data signals with (w/) and without (w/o) 150-W PWoF feed as a function of received electrical signal power.

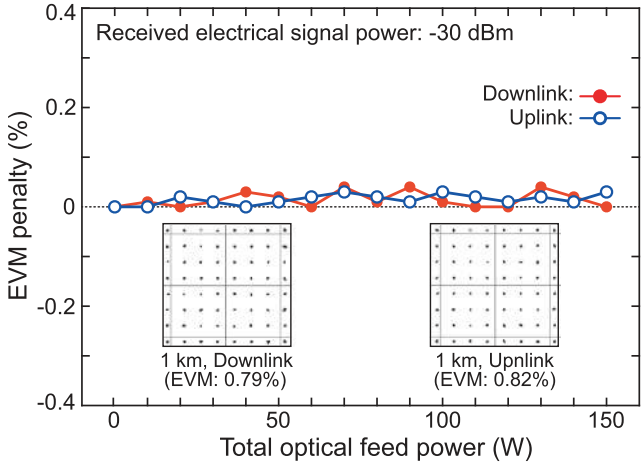


Fig. 9. EVM penalties to back-to-back signal of downlink- and uplink-transmitted data signals as a function of total optical feed power. Insets show constellations of downlink- and uplink-transmitted data signals with 150-W PWoF feed.

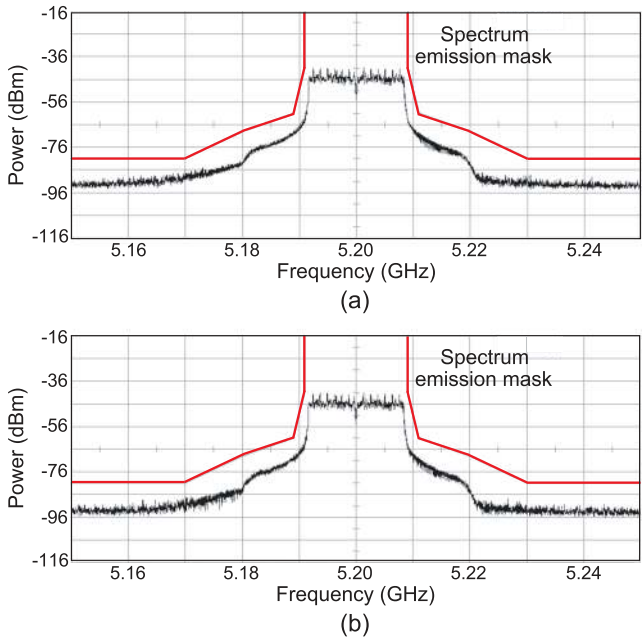


Fig. 10. SEMs of (a) back-to-back and (b) downlink-transmitted data signals with 150-W PWoF feed in 1-km DCF link.

the received power was larger than −30 dBm, the EVM values were almost constant at around 0.8%. Furthermore, the total optical feed power was no significant difference in the EVM characteristics. This result indicates that the combination of the high-power feed and the bidirectional transmission had very little effect on the transmission performance of the data signals in the DCF link.

Fig. 9 shows the EVM penalties to the back-to-back signal of the downlink- and uplink-transmitted data signals as a function of total optical feed power when the received electrical power was set to −30 dBm. Even when the total optical feed power was increased to 150 W, the EVM penalties did not increase and were almost constant at around 0.0%. The maximum EVM penalty was 0.04%. The insets show the constellations of the downlink- and uplink-transmitted data signals when the total optical power was set to 150 W. The EVM values were 0.79% and 0.82% for the downlink- and uplink-transmitted data signals, respectively.

To investigate the effect of the high-power feed on the transmitted signals in the electrical spectrum domain, we also measured the SEMs of the back-to-back and transmitted signals over the 1-km DCF link. Fig. 10 shows the SEMs of the downlink-transmitted signals for the 150-W PWoF feed. It was found that there was no significant difference in the SEMs of the both signals, and the signals had high relative power between the in-channel and out-of-channel emission.

At this point, we have reported some PWoF experiments with different feed optical powers of up to 60 W and transmission lengths of up to 300 m, and we have successfully achieved transmission performances equivalent to those of our previous experiments [15]−[22]. We found that the simultaneously transmitted data signals showed good transmission performances, even the 1-km transmission performed under the 150-W PWoF

feed. This result indicates that the presented PWoF system using DCFs has high potential for simultaneous data and power transmission lines in RoF networks.

## VII. Discussion

In this work, we focused on exploring the possibilities of the PWoF technique using a DCF for 150-W power feed, which is much higher than those of our previous works. Although the electrical power transmitted by the 150-W PWoF feed was approximately 7 W in this experiment, it is necessary to increase the transmitted electrical power. First, to do this, it is very important to improve the O/E conversion efficiency of PPCs. In this experiment, the silicon-based PPCs that we used have their highest O/E conversion efficiencies within a wavelength range between 900 nm and 980 nm [26], [27], which was the outside the suitable wavelength of the feed light source at 808 nm. Then, the O/E conversion efficiency was approximately 24%. On the other hand, conventional GaAs-based PPCs have their highest O/E conversion efficiencies with a wavelength range between 800 nm and 850 nm, which corresponds to the operating wavelength of the feed light source we used. Indeed, in the wavelength range, there are commercially available GaAs-based PPCs with O/E conversion efficiencies of up to 50% [29], and a few high-performance PPCs with O/E conversion efficiencies of up to 60% have been reported recently [30]–[32]. Therefore, it is expected that these PPCs will significantly contribute to increases in transmitted electrical power of PWoF systems in future. In addition, it is important to match the output voltage of PPCs with the voltage for driving RAUs. In this experiment, the output voltage of the PPCs at the highest O/E conversion efficiency was 18.5 V. However, it is possible to generally control the output voltage by varying the number of photovoltaic cells in PPCs [27], [33], we think that this problem can be easily solved by using suitable PPCs. The other approach is to improve the PTE of the PWoF system. In particular, it is important to reduce loss during the process of extracting the feed light from the inner cladding of the DCF. In the presented PWoF systems, as the data signals and feed light were divided by the TFBD with the six MMF outputs, the residual feed light component in the inner cladding had to be absorbed by the CPS at the output of the TFBD. If the number of the MMF outputs is increased, it will be possible to reduce the loss of the TFBD. We think that these approaches contribute to the significant improvement of the transmitted electrical power.

While we demonstrated the transmission experiments with the PWoF system in a DCF link of up to 1 km in length, it would be desirable to expand the transmission distances beyond this range. To do this, the wavelength of the feed light is important for suppressing the possible increase in the transmission loss of the DCF link. Indeed, the extension of the transmission distance from 300 m to 1 km drastically reduced the PTE of the feed light at a wavelength of 808 nm, because the transmission loss was 3.3 dB/km. In addition, to transmit as much electrical power as possible, it is also important that the O/E conversion efficiency of PPCs is dependent on wavelength. As we mentioned above, the silicon-based PPCs that we used have their highest O/E conversion efficiencies within a wavelength range between 900 nm and 980 nm, whereas conventional GaAs-based PPCs have their highest O/E conversion efficiencies with the range from 800 nm to 850 nm. Also, PPCs operating in other wavelength bands at 1550 nm [34] and 1310 nm [35] have also been reported. For PWoF systems with a longer transmission distance, the feed light wavelength should be carefully selected depending on the link length and the O/E conversion efficiency of the PPCs.

The development of optical power supply systems using optical fibers has good potential for supplying power to many types of equipment that until now could not be operated. Thus, further improvement in supplied power is useful for exploring new applications. For example, optically powered drones for airborne RAUs are potentially interesting applications. In future wireless communications, using airborne RAUs would enables us to enhance the capacity and coverage of mobile services for large number of audiences at major events, and would act to maintain mobile services as substitutes for ground RAUs that could be damaged in the event of natural disasters such as earthquakes. Conventional drones with batteries are not suitable for use as airborne RAUs owing to their limited flight times. However, optically powered drones that utilize optical fibers can remain in the air for unlimited durations. To show the preliminary feasibility of the drone, we performed a flight demonstration of an entry-type drone [36]. Although there are many issues that still need to be resolved, we believe that the challenges are technological in nature, and it is expected that they could be overcome in the near future.

## VIII. Conclusion

In this paper, we presented the simultaneous data and power transmission using a 1-km DCF. The transmitted feed light power of up to 150 W was converted electrical power using multiple PPCs in an RAU. We measured the bend performance and temperature change of the DCF link. In both cases, we showed the practicability of the presented PWoF system. We also successfully achieved good transmission performance for the downlink- and uplink-transmitted signals in the 150-W PWoF feed. The obtained results indicated that the PWoF technique using DCFs could be useful for future RoF networks.

## References

[1] D. Nesset, "NG-PON2 technology and standards," *J. Lightw. Technol.*, vol. 33, no. 5, pp. 1136–1143, Mar. 2015.

[2] I. A. Alimi, A. L. Teixeira, and P. P. Monteiro, "Toward an efficient C-RAN optical fronthaul for the future networks: A tutorial on technologies, requirements, challenges, and solutions," *IEEE Commun. Surv. Tuts.*, vol. 20, no. 1, pp. 708–769, Jan./Mar. 2018.

[3] J. Cooper, "'Fiber/radio' for the pr–ovision of cordless/mobile telephony services in the access network," *Electron. Lett.*, vol. 26, no. 24, pp. 2054–2056, Nov. 1990.

[4] M. Sauer, A. Kobyakov, and J. George, "Radio-over-fiber for picoceller network architectures," *J. Lightw. Technol.*, vol. 25, no. 11, pp. 3301–3320, Nov. 2007.

[5] C. Liu, J. Wang, L. Cheng, M. Zhu, and G. Chang, "Key microwave-photonics technologies for next-generation cloud-based radio access networks," *J. Lightw. Technol.*, vol. 32, no. 20, pp. 3452–3460, Oct. 2014.

[6] I. Ashraf, F. Boccardi, and L. Ho, "SLEEP mode techniques for small cell deployments," *IEEE Commun. Mag.*, vol. 49, no. 8, pp. 72–79, Aug. 2011.

[7] K. Sone, I. Kim, X. Wang, Y. Aoki, H. Seki, and J. C. Rasmussen, "Analysis of power consumption in mobile Backhaul network with densely deployed small cells under dynamic traffic behavior," in *Proc. Opto-Electron. Commun. Conf. Photon. Switching*, Niigata, Japan, Jul. 2016, Paper TuA4-2.
[8] J. Wu, Y. Zhang, M. Zukerman, and E. K.-N. Yung, "Energy-efficient base-stations sleep-mode techniques in green cellular networks: A survey," *IEEE Commun. Surv. Tuts.*, vol. 17, no. 2, pp. 803–826, Apr./Jun. 2015.
[9] M. Matsuura, "Power-over-fiber technologies for radio-over-fiber-based distributed antenna systems," in *Proc. Pacific Rim Conf. Lasers Electro-Opt.*, Hong Kong, Aug. 2018, Paper Th4F.2.
[10] T. Miki, K. Kawano, N. Nakajima, N. Kishi, M. Miyamoto, and T. Aoki, "Novel radio on fiber access eliminating electric power supply at base station," in *Proc. Opto-Electron. Commun. Conf.*, Shanghai, China, Jul. 2003, Paper 16D3-4.
[11] D. Wake, A. Nkansah, N. J. Gomes, C. Lethien, C. Sion, and J.-P. Vilcot, "Optically powered remote units for radio-over-fiber systems," *J. Lightw. Technol.*, vol. 26, no. 15, pp. 2484–2491, Aug. 2008.
[12] C. Lethien *et al.*, "Energy-autonomous picosecond remote antenna unit for radio-over-fiber system using the multiservice concept," *Photon. Technol. Lett.*, vol. 24, no. 8, pp. 649–651, Apr. 2012.
[13] H. Kuboki and M. Matsuura, "Optically powered radio-over-fiber system based on center- and offset-launching techniques using a conventional multimode fiber," *Opt. Lett.*, vol. 43, no. 5, pp. 1057–1070, Mar. 2018.
[14] A. Ikukawa, H. Kuboki, and M. Matsuura, "Relative phase noise evaluation of power-over-fiber in multimode fibers," in *Proc. 1st Opt. Wireless Fiber Power Transmiss. Conf.*, Yokohama, Japan, Apr. 2019, Paper OWPT-P-09.
[15] J. Sato and M. Matsuura, "Radio-over-fiber transmission with optical power supply using a double-clad fiber," in *Proc. Conf. Lasers Electro-Opt. Pacific Rim, Opto-Electron. Commun. Conf./Photon. Switching*, Kyoto, Japan, Jul. 2013, Paper TuPO-8.
[16] M. Matsuura and J. Sato, "Bidirectional radio-over-fiber systems using double-clad fibers for optically powered remote antenna units," *IEEE Photon. J.*, vol. 7, no. 1, Feb. 2015, Art. no. 7900609.
[17] J. Sato, H. Furugori, and M. Matsuura, "40-Watt power-over-fiber using a double-clad fiber for optically powered radio-over-fiber systems," in *Proc. Opt. Fiber Commun. Conf. Expo.*, Los Angeles, USA, Mar. 2015, Paper W3F.6.
[18] M. Matsuura, H. Furugori, and J. Sato, "60 W power-over-fiber feed using double-clad-fibers for radio-over-fiber systems with optically powered remote antenna units," *OSA Opt. Lett.*, vol. 40, no. 23, pp. 5598–5601, Dec. 2015.
[19] A. Yoneyama, Y. Minamoto, and M. Matsuura, "Power-over-fiber transmission using 1.3-$\mu$m dual-channel radio-over-fiber signals in a double-clad fiber," in *Proc. Opto-Electron. Commun. Conf. Int. Conf. Photon. Switching*, Niigata, Japan, Jul. 2016, Paper TuA2-4.
[20] M. Matsuura and Y. Minamoto, "Optically powered and controlled beam steering system for radio-over-fiber networks," *J. Lightw. Technol.*, vol. 35, no. 4, pp. 979–988, Feb. 2017.
[21] D. Kamiyama, A. Yoneyama, and M. Matsuura, "Multichannel data signals and power transmission by power-over-fiber using a double-clad fiber," *Photon. Technol. Lett.*, vol. 30, no. 7, pp. 646–649, Apr. 2018.
[22] M. Matsuura, "Optically powered radio-over-fiber systems," in *Proc. Conf. Lasers Electro-Opt.*, San Jose, CA, USA, May 2018, Paper SM1C.3.
[23] N. Tajima, A. Yoneyama, D. Kamiyama, and M. Matsuura, "Over 1-km power-over-fiber using a double-clad fiber for bidirectional RoF systems," in *Proc. Opto-Electron. Commun. Conf.*, Jeju, Korea, Jul. 2018, Paper 4A4-2.
[24] N. Tajima, D. Kamiyama, and M. Matsuura, "150-Watt power-over-fiber feed for bidirectional radio-over-fiber systems using a double-clad fiber," in *Proc. Opt. Fiber Commun. Conf. Expo.*, W1I.7, San Diego, CA, USA, Mar. 2019.
[25] M. Matsuura, "Over 100-W power-over-fiber for remote antenna units," in *Proc. 1st Opt. Wireless Fiber Power Transmiss. Conf.*, Yokohama, Japan, Apr. 2019, Paper OWPT-5-01.
[26] M. Perales *et al.*, "Characterization of high performance silicon-based VMJ PV cells for laser power transmission applications," *Proc. SPIE*, vol. 9733, Jan. 2016, Art. no. 97330U.
[27] M. Perales, "Low cost laser power beaming and power over fiber systems," in *Proc. 1st Opt. Wireless Fiber Power Transmiss. Conf.*, Yokohama, Japan, Apr. 2019, Paper OWPT-7-01.
[28] A. A. P. Boechat, D. Su, D. R. Hall, and J. D. C. Jones, "Bend loss in large core multimode optical fiber beam delivery systems," *Appl. Opt.*, vol. 30, no. 3, pp. 321–327, Jan. 1991.
[29] Broadcom Inc., Optical power converters. 2019. [Online]. Available: https://www.broadcom.com/products
[30] O. Höhn, A. W. Walker, A. W. Bett, and H. Helmers, "Optimal laser wavelength for efficient laser power converter operation over temperature," *Appl. Phys. Lett.*, vol. 108, no. 24, Jun. 2016. Art. no. 241104.
[31] S. Fafard *et al.*, "High-photovoltage GaAs vertical epitaxial monolithic heterostructures with 20 thin p/n junctions and a conversion efficiency of 60%," *Appl Phys. Lett.*, vol. 109, no. 13, Sep. 2016, Art. no. 131107.
[32] S. Fafard *et al.*, "Ultrahigh efficiency optical power converters based on the vertical epitaxitial heterostructure architecture (VEHSA) design," in *Proc. 1st Opt. Wireless Fiber Power Transmiss. Conf.*, Yokohama, Japan, Apr. 2019, Paper OWPT-3-01.
[33] J.-G. Werthen, "Powering next generation networks by laser light over fiber," in *Proc. Conf. Opt. Fiber Commun./Nat. Fiber Optic Eng. Conf.*, San Diego, USA, Mar. 2008, Paper OWO.3.
[34] S. J. Sweeney, S. D. Jarvis, and J. Mukherjee, "Laser power converters for eye-safe optical power delivery at 1550 nm: Physical characteristics and thermal behavior," in *Proc. 1st Opt. Wireless Fiber Power Transmiss. Conf.*, Yokohama, Japan, Apr. 2019, Paper OWPT-2-04.
[35] M. M Wilkins *et al.*, "Progress towards vertically stacked InAlGaAs photovoltaic power converters for fiber power transmission at 1310 nm," in *Proc. 1st Opt. Wireless Fiber Power Transmiss. Conf.*, Yokohama, Japan, Apr. 2019, Paper OWPT-2-05.
[36] R. Yazawa and M. Matsuura, "Optically powered drone small cells using optical fibers," *IEICE Electron. Express*, vol. 15, no. 10, May 2018, Art. no. 20183271.

**Motoharu Matsuura** (M'04−SM'13) received the Ph.D. degree in electrical engineering from the University of Electro-Communications, Tokyo, Japan, in 2004. He joined the Department of Information and Communication Engineering, University of Electro-Communications as an Assistant Professor in 2007. From 2010 to 2011, on leave from the university, he joined the COBRA Research Institute, Eindhoven University of Technology, Eindhoven, The Netherlands, as a Visiting Researcher, where he studied ultrahigh-speed optical signal processing using semiconductor-based devices. He is currently a Professor with the Graduate School of Informatics and Engineering, University of Electro-Communications. He has been researching optical signal processing, photonic subsystems, and radio-over-fiber transmission systems. He is the Author or Coauthor of more than 200 papers published in international refereed journals and conferences, including OFC and ECOC Postdeadline Papers and OFC Top Scored Papers. He received the Ericsson Young Scientist Award in 2008, the FUNAI Information Technology Award for Young Researcher in 2009, and Telecommunication System Technology Award of the Telecommunications Advancement Foundation in 2011. He is a Member of the Optical Society of America and the Institute of Electronics, Information and Communication Engineers.

**Nana Tajima** received the B.E. degree from Yamagata University, Yamagata, Japan, in 2017, and the M.E. degree from the University of Electro-Communications, Tokyo, Japan, in 2019, respectively, She joined NTT Docomo Inc., Tokyo, Japan, in 2019. Her research interests include radio-over-fiber transmission systems and the subsystems.

**Hayato Nomoto** received the B.E. degree from the University of Electro-Communications, Tokyo, Japan, in 2019. He is currently working toward the master's degree with the University of Electro-Communications. His research interests include radio-over-fiber transmission systems and the subsystems.

**Daisuke Kamiyama** received the B.E. and M.E. degrees from the University of Electro-Communications, Tokyo, Japan, in 2017 and 2019, respectively. He joined NTT Docomo Inc., Tokyo, Japan, in 2019. His research interests include radio-over-fiber (RoF) transmission systems and the subsystems.